Submicron Optical Lithography Based on a New Interferometric Phase Shifting Technique



1995 Jpn. J. Appl. Phys. 34 4269

(http://iopscience.iop.org/1347-4065/34/8R/4269)

Jpn. J. Appl. Phys. Vol. 34 (1995) pp. 4269–4273
Part 1, No. 8A, August 1995

# Submicron Optical Lithography Based on a New Interferometric Phase Shifting Technique

Motoi KIDO, Gabor SZABÓ[1] Joseph R. CAVALLARO, William L. WILSON, Michael C. SMAYLING[2] and Frank K. TITTEL

*Department of Electrical and Computer Engineering, Rice University, P.O. Box 1892, Houston, Texas 77251, USA*
[1]*Department of Optics and Quantum Electronics, JATE University, H-6720 Szeged, Hungary*
[2]*Texas Instruments Inc., Stafford, Texas 77477, USA*

(Received March 22, 1995; accepted for publication May 22, 1995)

This paper reports the computer simulation and experimental demonstration of a new phase shifting technique based on interferometry that is especially suited for deep ultraviolet (UV) microlithography. Significant resolution and contrast enhancement can be achieved using a chrome binary mask. Image analysis based on charge coupled device (CCD) detection and patterns recorded in UV photoresist has been used to study the capabilities of this new approach. Lines with a feature size as fine as 0.3 $\mu$m have been demonstrated using 355 nm illumination.

KEYWORDS: phase shifting technique, deep-UV microlithography

## 1. Introduction

Advanced optical microlithography will be needed in order to achieve the smaller size features required by future high density integrated circuit designs.[1-3] Since the critical feature size ($W$) can be expressed as

$$W = (k_1 \cdot \lambda)/NA\,, \tag{1}$$

where $\lambda$ is the wavelength, $NA$ is the numerical aperture of the imaging system, and $k_1$ is a numerical parameter characteristic of a given optical system, a common strategy for achieving smaller feature size has been to increase the $NA$ of the exposure tool. This approach is effective as long as the amount of defocus that can be tolerated is sufficiently large. Although this tolerance depends upon the shape of the pattern to be printed, the photoresist and several other processing parameters, it is evident that axial variables cannot be neglected. As $W$ is shrunk to half micron and below it has been recognized, that depth of focus ($DOF$) also becomes a critical variable.[4] Since $DOF$ can be expressed as

$$DOF = (k_2 \cdot \lambda)/NA^2\,, \tag{2}$$

where $k_2$ is also an empirical parameter, it is clear that once the defocus tolerances are given, an upper bound for the useful $NA$ is established. Thus, one possible solution to achieve even smaller feature size is to decrease $k_1$ and keep $NA$ constant. Phase shifting (PS) is considered an effective technique for making $k_1$ smaller and, in recent years, different phase shifting methods have been proposed.[5-8]

This paper describes a new approach to phase shifting that does not require any special "optically thick" phase shifting elements to be incorporated into the mask. Rather, the technique uses a conventional single-layer chrome mask in a unique interferometric illumination arrangement. The basic scheme is shown in Fig. 1. A one-layered chrome reticle is used as both a reflective and a transmissive element. An incoming laser beam is divided by a beam splitter. These beams illuminate the mask from both the front and back side via an additional beam splitter and mirror as shown. The reflected and transmitted beams are then colinearly combined and imaged onto the substrate. The optical paths of the beams are chosen so that the phase of the two beams differs by an odd multiple of $\pi$ radians at the surface of the mask. This is accomplished by adjustment of the position of the mask to achieve the desired phase shifting effect, as illustrated in Fig. 2. The two out-of-phase beams cancel each other when they overlap, resulting in higher contrast and resolution than is possible with conventional projection lithography. It is important that the overall path difference between the two beams be less than the coherence length of the illumination source, in order to achieve the desired interferometric effect. The proposed scheme can be used with both conventional light sources as well as laser illumination. The optical characteristics of the actual mask substrate should be such as to maintain phase uniformity over the overall effective target area.

By using this approach, any phase shifting concept such as chromeless, attenuated, or rim shifting can be realized. In the experiments described below, an arrangement was tested that is equivalent to the chromeless phase-shifting method.[9,10] The essential difference is that a conventional chrome mask is used instead of the more difficult to fabricate, multi-layer dielectric mask.

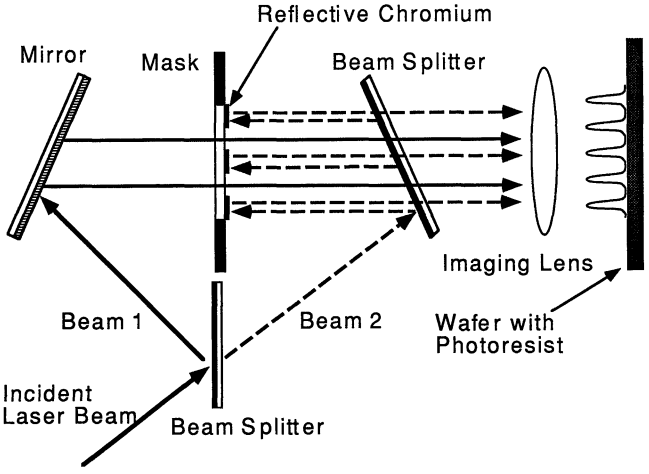


Fig. 1. Scheme of the new phase shifting method based on interferometry.

This new phase shifting method is particularly useful for short wavelengths, such as KrF illumination at 248 nm,[11,12] or ArF at 198 nm, where it becomes increasingly difficult to find appropriate materials with which to fabricate the phase shifting elements.

## 2. Simulations

To confirm and evaluate the performance of this new approach, the conventional transmission method, the standard phase shifting method[6,13-15] and the new interferometric method were simulated using the DEPICT[16] photolithography simulator. Alternating clear and opaque lines were used to model the conventional transmission approach. These were changed to include a 180° phase shift in alternating clear regions to model the standard-type phase shifting approach. To model the new method, only clear lines were used, with a 180° phase shift inserted for each neighboring line. The lines with 0° phase shift were used to model the transmitting regions of the mask, while the lines with 180° phase shift corresponded to the reflecting regions of the mask. Because illumination from a laser with a stable mode resonator was being modeled, spatial coherence was assumed. Several different wavelengths and mask dimensions were investigated. The imaging lens was assumed to have a numerical aperture of 0.4. The partial coherence ($\sigma$) of the illumination system was modeled to be $\sigma \approx 0.2$ based on the experimental setup. The small diameter laser beam illuminated the mask and was then imaged with a microscope objective lens. Simulations were performed for $0.05 \leq \sigma \leq 0.9$ and nearly constant contrast results were obtained for $0.05 \leq \sigma \leq 0.4$. An example for a wavelength of 457 nm is shown in Fig. 3. The figure clearly demonstrates that the new phase mask offers the same performance as a chromeless mask.

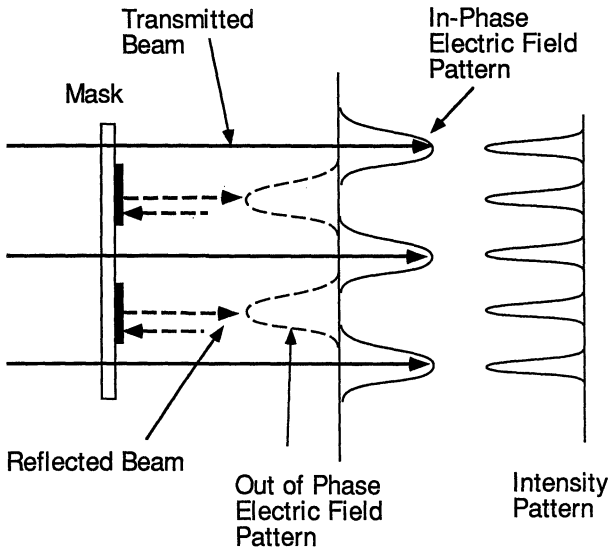


Fig. 2. Phase shifting effects obtained by interferometry using a one-layered metal mirror type mask.

By rearranging eq. (1), we can see that the physical meaning of $k_1$ is the normalized minimum feature size,[17] i.e., the minimum feature size measured in units of illumination wavelength. The normalized minimum feature size is a fundamental figure of merit for lithographic techniques and, therefore, it provides an illustrative basis to compare the performance of different phase shifting arrangements. Since the definition of resolution limit is somewhat arbitrary and depends on several parameters such as the type of resist used, it is possible to compare the optical characteristics of the different methods in terms of the contrast ($C$) of the final image as a function of the normalized feature size ($k_1$). Usually, the contrast is defined[18] as

$$C = (I_{\text{peak}} - I_{\text{min}})/(I_{\text{peak}} + I_{\text{min}}) , \qquad (3)$$

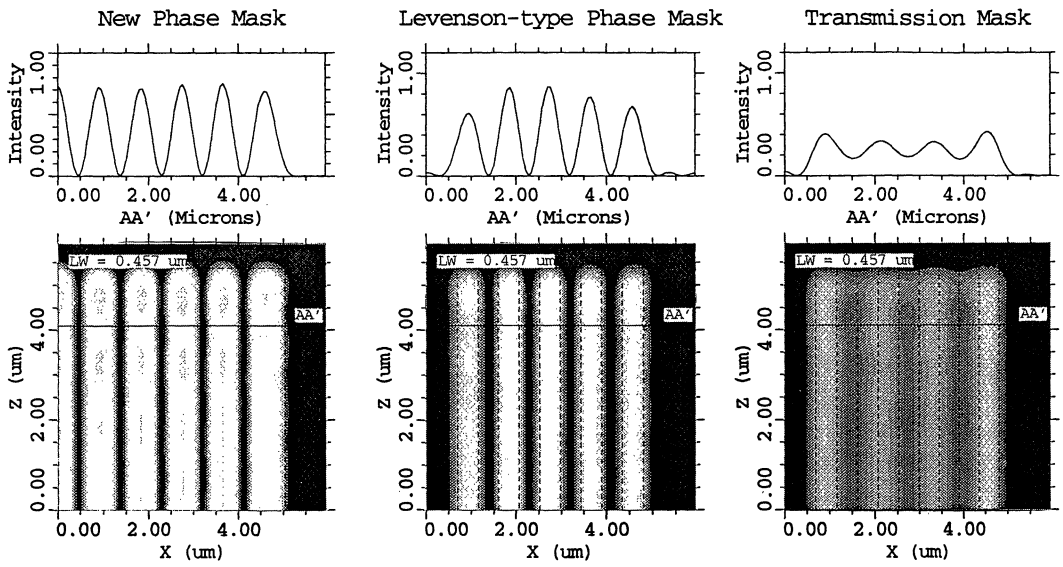


Fig. 3. Example of DEPICT results. One dimensional and two dimensional light intensity distributions for a line and space pattern are shown for the new phase shifting method, compared with the conventional Levenson type phase shifting method and a transmission mask. A one dimensional intensity profile along the line (AA′) is extracted from the two dimensional simulation data. A wavelength of 457 nm, partial coherence of 0.2, image period of 0.914 $\mu$m, $NA$ of 0.4 and optimum focus are used as the optical input parameters.

where $I_{peak}$ is the intensity at the peak of the pattern and $I_{min}$ is the intensity at its minimum. The contrast alone, however, is somewhat misleading in favor of PS techniques when compared with conventional lithography. This is because for images formed by the PS technique, $I_{min}$ remains nearly zero, while $I_{peak}$ decreases as the feature size is reduced. With $I_{min} \approx 0$, the contrast is nearly 100%, even though the quality of the resultant image is seriously degraded and the intensity at the surface of the wafer is low. In order to take this effect into account when evaluating different photolithographic techniques, a performance index ($PI$) is introduced, where

$$PI = I_{peak} C \,. \tag{4}$$

The $PI$ takes into account the peak intensity of the image, as well as its contrast and, in this case, it is a better measure of image quality than contrast alone.

Figure 4 shows the results of DEPICT simulations of all three photolithographic techniques, where the performance index $PI$ is plotted as a function of $W \cdot NA/\lambda$. Both PS approaches show significant advantages over the conventional transmission mask performance. As can be seen, the performance index of the transmission mask decreases rapidly for $W \cdot NA/\lambda$ less than about 0.5, which is to be expected when the Rayleigh resolution limit is considered in eq. (1). The performance index for both phase shifting approaches remains high for $W \cdot NA/\lambda$ down to about 0.26. This corresponds to a minimum feature size of about 0.2 $\mu$m for KrF (248 nm) illumination with $NA = 0.32$. The simulated performance index of the new phase shifting method shows a slight increase for $W \cdot NA/\lambda \sim 0.3$. This peak is caused by the second order Airy pattern peak that has an electric field of opposite sign from the primary peak. This field contributes to the electrical field intensity of the neighboring phase shifted line, and increases its performance index. With this phase shifting technique, the image contrast remains high, even though the intensity tends to decrease near critical resolution. It may be possible to take advantage of this improved performance around $W \cdot NA/\lambda$ of 0.3 to enhance the image near critical resolution.

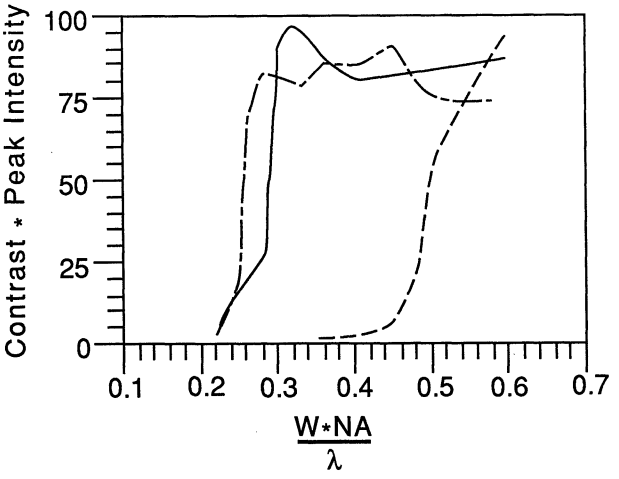


Fig. 4. Comparison of the product of contrast times peak intensity for the new phase shifting method (—), Levenson-type phase shifting method (– – –), and transmission approach (- - - -) as a function of linewidth $W$ normalized by the ratio of $\lambda/NA$ using DEPICT. A wavelength of 457 nm, partial coherence of 0.2 for laser illumination, and a $NA$ of 0.4 are used as optical input parameters.

In this simulation, alignment errors and aberrations in the optics were neglected. In practice, however, these errors could become important. Alignment errors caused by the position of the imaging lens and the silicon wafer are the same as in conventional PS and transmission mask approaches. A mask positioning error that determines the difference of the optical paths and thereby the amount of phase shift between the two beams is a parameter special to this method. The positioning parameter, however, can be controlled by some relatively simple servo mechanism. The reference signal of such a servo controller can, for instance, be provided by measuring the intensity from a reference pad on the mask with sub-resolution features. Areas with sub-resolution features are expected to appear as dark regions assuming 180° phase difference.[19] Thus, the control parameter of the servo system could be the intensity minimum of such reference pads. The fact that the phase difference can be controlled is one of the main advantages of the new PS method. Phase errors that occur during manufacturing can cause serious difficulties in conventional phase masks, since they are turned into focusing offsets by the imaging system.[19] In the interferometric PS technique this effect is dynamically suppressed.

Strong PS techniques (such as the Shibuya-Levenson type) offer significant resolution and $DOF$ advantages, but they are prone to phase conflicts that may lead to fundamental design issues that can be solved by subshifters, or by a second exposure with a block-out mask.[19,20] Attenuated PS techniques,[21] on the other hand, are less effective in improving resolution, but they are considered to be universally applicable. In practical implementation of attenuated PS concepts, however, it is important to fabricate layers that provide the necessary phase shifting and transmission at the same time, which makes fabrication difficult at UV wavelengths. By using the interferometric PS technique, any intensity ratio between the two interfering beams can be obtained and, thus, the attenuated PS concept can be readily implemented with a simple chrome reticle. Furthermore, the weak interferometric PS technique lends itself to be combined with off-axis illumination that can be used as an effective exposure tool with $k_1 = 0.5$.[20,22]

## 3. Experiments and Discussion

A series of experiments were carried out in order to evaluate the feasibility and performance characteristics of this new approach to phase shifting. A charge coupled device (CCD) camera was used to quantify the intensity distribution pattern generated by the new method. Additionally, patterns were written onto Hoechst Celanese AZ1350B-SF photoresist with two different continuous (CW) lasers and one pulsed laser source. The first coherent source was a 1 mW He-Ne laser (632.8 nm, $TEM_{00}$ mode, 0.8 mm beam diameter). After initial tests, this source was replaced with a 100 mW single frequency $Ar^+$ laser (457 nm, $TEM_{00}$ mode, 1.4 mm beam diameter).

To study pulsed UV illumination, we used a Nd:YAG laser (operated at 355 nm using third harmonic generation, 2.0 mJ, with a pulse duration of 10 ns and a repetition rate of 10 PPS). The experimental setup is shown in Fig. 5. A 20× microscope objective lens with a 0.4 *NA* was used as the imaging lens for visible laser experiments. Similarly, a 20× objective with UV transmitting glass and a 0.5 *NA* was used for UV laser illumination experiments. The mask consisted of a single layer of chrome with a number of different line and space patterns. Patterns with line size ranging from 2 to 22 $\mu$m could be selected. A neutral density filter (density 0.3) was placed in the transmitting branch in order to equalize the beam intensities. A CCD camera system with a 0.8 *NA* and magnifying optics that expanded the focused image onto the CCD image plane was used to evaluate the projected pattern. Each CCD pixel corresponded to about 0.01 $\mu$m in the focused image plane. Beam profiling software was used to analyze the intensity distribution at the image plane.

The measured *PI* is depicted in Fig. 6. Squares, triangles, and diamonds represent the measured points at 632 nm, 457 nm, and 355 nm respectively, while the results of the DEPICT simulation are given by dashed line. At 632 nm, the experimental data and the DEPICT simulation agree well. In both the experiment as well as the simulation, line widths corresponding to a $W \cdot NA/\lambda$ of slightly less than 0.27 (corresponding to a feature size of about 0.66 $\lambda$) were achievable. At 457 nm, the experimental results showed slightly reduced resolution, with a minimum $W \cdot NA/\lambda$ of about 0.3 (corresponding to a 0.75 $\lambda$ feature size). However, for pulsed 355 nm UV experiments using the third harmonic of a Nd:YAG laser (with a bandwidth of ~30 GHz), the measured *PI* is reduced corresponding to a minimum $W \cdot NA/\lambda$ of about 0.4 (feature size of 0.8 $\lambda$). This reduction in *PI* is not inherent to the method but is mainly caused by the beam quality of the Nd:YAG laser at our disposal.

Patterns were also written on AZ1350B-SF UV photoresist. During the photoresist exposure, the CCD camera was used to observe the reflected image from the silicon wafer in order to aid in alignment. The photoresist development simulation capability of DEPICT was used to estimate the required exposure fluences. The simulations indicated a target exposure energy density of approximately 150 mJ/cm$^2$ at 457 nm and 60 mJ/cm$^2$ at 355 nm.

Experiments were conducted using the UV photoresist at both 457 nm and 355 nm. A layer of photoresist approximately 0.5 $\mu$m thick was deposited on a 1.5 inch diameter silicon wafer by spinning the wafer at 3000 rpm. At 457 nm, a laser beam intensity density of 50 mW/cm$^2$ was used to expose the wafer for 4 s, resulting in a deposited energy density of 200 mJ/cm$^2$ in the photoresist. This produced a 0.57 $\mu$m wide line pattern in the resist. The frequency tripled Nd:YAG exposure at 355 nm consisted of a train of 5 pulses, with a pulse duration of 10 ns, having a total deposited energy density of 30 mJ/cm$^2$. Figure 7 is a scanning electron microscope (SEM) photograph of the features obtained using UV laser illumination. A line size of $\leq$ 0.3 $\mu$m

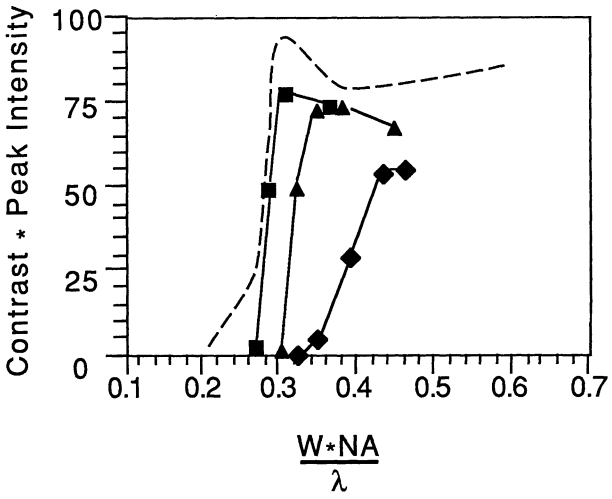


Fig. 6. Comparison of image contrast times peak intensity between a DEPICT simulation (----) and experiments with 632.8 nm (–□–), 457 nm (–△–), and 355 nm (–◇–) laser illumination as a function of linewidth $W$ normalized by $\lambda/NA$. A *NA* of 0.4 is used for the 632.8 nm and 457 nm experiments, and a *NA* of 0.5 is used for the 355 nm experiment as optical input parameters.

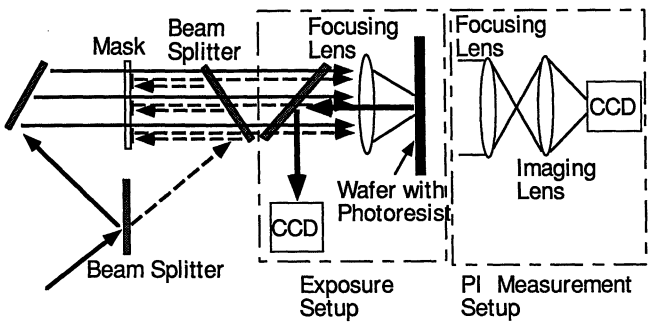


Fig. 5. Schematic of the experimental setup. Photoresist exposure experiment setup (left column) and performance measurement setup (right column) are shown in this figure.

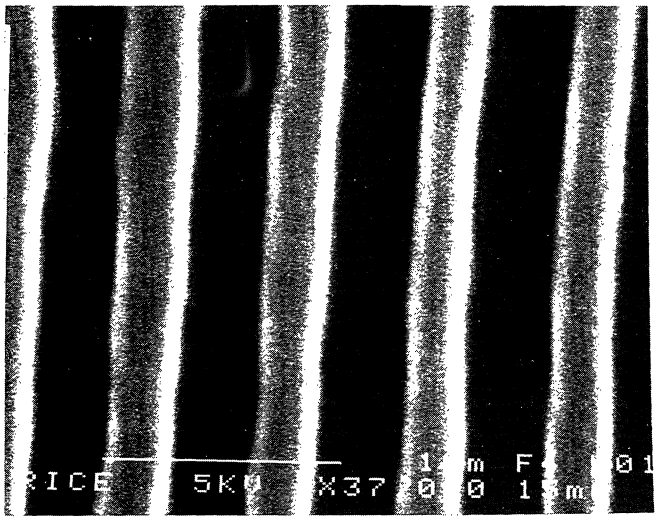

Fig. 7. SEM photograph of pattern features of 0.30 $\mu$m linewidth produced by interferometric phase shifting scheme with 355 nm laser illumination.

was obtained, which demonstrates the capability of this new phase shifting method. The depth of the photoresist patterns was measured with an atomic force microscope (AFM) and found to be 0.4 $\mu$m.

## 4. Conclusions

The performance of a new phase shifting method suitable for the fabrication of high density dynamic random access memory (DRAM) IC's has been demonstrated, based on an interferometric scheme and a single layer chrome mask. The scheme has been modeled using the DEPICT photolithographic simulator, and critical error tolerances were analyzed and compared to the experimentally obtained data. A line and space pattern mask was used in a 20× reduction scheme to write 0.3 $\mu$m thick lines in UV photoresist with light from a 355 nm frequency tripled Nd:YAG laser. A distinct advantage of this phase shifting method is that the amount of phase shift and the relative intensity of the two out-of-phase images can be independently controlled and adjusted. Because the image which is created at the wafer surface is the same as that which would be formed using a chromeless phase-shift mask, similar advantages in terms of *DOF* and resolution are anticipated.[5] Line features as small as 0.2 $\mu$m should be feasible with a 248 nm KrF excimer laser based photolithographic stepper. Hence, this new phase shifting technique can potentially provide the 0.25 $\mu$m technology that will be required for the fabrication of 256 Mbit DRAM's.

## Acknowledgements

The authors would like to thank Professor D. Callahan for helpful suggestions for the SEM measurements, and Technology Modeling Associates for the DEPICT simulator. This research was supported in part by NSF under grant DDM/DMI-9202639.

1) D. J. Ehrlich and J. Y. Tsao: *Laser Microfabrication* (Academic Press, 1989).
2) M. Horiguchi *et al.*: 1995 IEEE Int. Solid State Circuits Conf. Proc., p. 255.
3) W. H. Arnold: Microlithogr. World **4** (1995) 7.
4) H. J. Levinson and W. H. Arnold: J. Vac. Sci. Technol. B **5** (1987) 293.
5) B.J. Lin: IEEE Circuits & Devices Mag. **2** (1993) 28.
6) M. Shibuya: Japanese Pat. No. Showa 62-50811 (30 Sept. 1980).
7) M. D. Levenson, N. S. Visnawathan and R. A. Simpson: IEEE Trans. Electron. Devices **29** (1992) 1828.
8) K. K. H. Toh: Proc. SPIE **1463** (1991) 402.
9) H. Watanabe, H. Takenaka, Y. Todokoro, and S. Okazaki: J. Vac. Sci. Technol. B **9** (1991) 3172.
10) K.K.H. Toh, G. Dao, R. Singh, and H. Gaw: Proc. SPIE **1496** (1990) 27.
11) K. Yamashita, M. Endo, M. Sasago, N. Nomura, H. Nagano, S. Mizuguchi, T. Ono and T. Sato: J. Vac. Sci. Technol. B **11** (1993) 2692.
12) U. K. Sengupta: Opt. Eng. **32** (1993) 2410.
13) R. L. Hsieh, Y. Y. Lee, N. I. Maluf, R. Browning, P. Jerabek and R. F. Pease: Proc. SPIE **1604** (1991) 67.
14) D. M. Newmark and A. R. Neureuther: Proc. SPIE **1604** (1991) 226.
15) Y. Liu, A. Pfau and A. Zakhor: IEEE Trans. Semicond. Manufact. **6** (1993) 1.
16) R. C. Pack and D. A. Bernard: DEPICT-2 Applications for VLSI Technology, Technical Report, Technology Modeling Associates Inc., Palo Alto, CA, USA (1990).
17) B.J. Lin: Proc. SPIE **1463** (1991) 42.
18) W. B. Glendinning and J. N. Helbert: *Handbook of VLSI* (Noyes Publications, Park Ridge, 1991) p. 239.
19) F. M. Schellenberg and M. D. Levenson: Proc. SPIE **1809** (1992) 237.
20) T.A. Brunner: Opt. Eng. **32** (1993) 2337.
21) B. Lin: Solid State Technol. **35** (1992) 43.
22) K. Kamon, T. Miyamoto, Y. Myoi, H. Nagata, N. Kotani and M. Tanaka: Jpn. J. Appl. Phys. **31** (1992) 4131.